Random Walks in the Model Brain Tissue: Monte Carlo Simulations and Implications for Diffusion Imaging

F. Grinberg[1], Y. Kupriyanova[1], A-M. Oros-Peusquens[1], and N. J. Shah[1,2]
[1]Medical Imaging Physics, Institute of Neuroscience and Medicine 4, Forschungszentrum Juelich GmbH, Juelich, Germany, [2]Department of Neurology, Faculty of Medicine, RWTH Aachen University, Aachen, Germany

Introduction

Diffusion MRI gives rise to unique opportunities in brain diagnostics and has become an indispensable tool in clinical applications. Conventional methods are based on a simplified picture of Gaussian diffusion characteristic of non-confined liquids. However, more detailed experiments show that water in brain tissue tends to exhibit essential deviations from patterns of Gaussian diffusion. The propagation of water molecules in the brain is affected by multiple factors such as compartmentalization, restrictions and anisotropy imposed by the cellular microstructure [1]. Interfacial interactions with the cell membranes ("bound water") and exchange may further complicate the measured response [2]. Due to the heterogeneity and complexity of tissue microstructure, a differentiation between the various contributions to the average NMR signal in *in vivo* studies represents a difficult task. The aim of this work is to conduct random-walk Monte Carlo simulations [3] in well-defined model systems and to establish the relations between dynamic properties and structure in a quantitative manner. A detailed analysis of the average diffusion propagator and the corresponding signal attenuation is performed. The results are compared with the *in vivo* data and the implications for the experimental studies are discussed.

Models and Methods

Three-dimensional random walks were simulated for a model system consisting of the parallel cylinders, Fig.1, immersed in a homogeneous, cubic space. In addition to regular geometrical models most frequently discussed in the literature [1], we also consider a randomly packed geometry that tends to resemble white-matter micrographs more closely. During the course of the total simulation time, T, the random walk repeatedly probes all sites within the system, including both the intra- and the extra-cylinder spaces denoted as ICS and ECS, respectively. T was several orders of magnitude larger than the "observation" time, t, to assure sufficient statistical averaging and accuracy. The intrinsic diffusivity, D_{intr} was equal to $1\times10^{-9}\,\mathrm{m^2s^{-1}}$. The evaluated quantities were the mean squared displacements $\langle \Delta x_i^2 \rangle$, the displacement profiles of the 3D average diffusion propagator $P(\Delta x_i, t)$, and the signal attenuation by diffusion $S_i(q)$ ($q = \gamma^2\delta^2 g^2$ is the wave vector) with respect to the different directions i. The effects of cylinder radius, R, cylinder size distribution, the packing density (i.e., the relative volume fractions of the ECS and ICS), and a cylinder-wall permeability were considered.

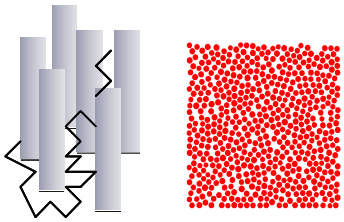

Figure 1. The geometrical model system.

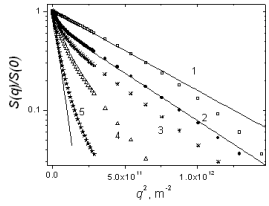

Figure 2. Examples of the diffusion attenuation curves (R=2.5 μm).

Results and Discussions

Figure 2 shows some examples of the attenuation curves for diffusion in the direction perpendicular to the long cylinder-axis. The curves refer to the localised motion in a single cylinder (curve 1), "hindered" motion in the ECS (curve 5), and diffusion in the whole system (ICS+ECS) in the limit of slow exchange (curve 2). Deviations from Gaussian behaviour were observed in all cases, including the individual compartments (ICS and ECS). For sufficiently small R, the two attenuation components are readily distinguishable for the whole system (curve 2). They can be roughly attributed to the contributions from the ECS (more essential in the range of low q, "fast" component) and the ICS (dominating at large q, "slow" component). At sufficiently high q-values, the "slow" component merely resembles localised motion (in the perpendicular direction) within the cylinders. Curves 3, 4 demonstrate the changes caused by increasing permeability of the walls. These changes appear more pronounced in the slow component. Figure 3 shows the reduced diffusivity, D_{red}, evaluated from the initial slopes of the simulated attenuations as a function of R (slow-exchange limit). The power law dependence $\propto 0.3R^2$ for localised motion within a cylinder is clearly observed in accordance with analytical expectations. In the ECS and in the whole system, the dependence $D_{red}(R)$ is more shallow and is affected by additional geometrical features such as packing geometry and the relative ECS volume. In conclusion, diffusion measurements at high q are required for better quantification of the confinement size. Simulations have shown that a differentiation between the ICS and ECS is possible only for R below a certain (rather small) threshold value which depends on the observation time. Time-dependent diffusion measurements, in turn, are necessary in order to discriminate the effects of restrictions and exchange in *in vivo* studies.

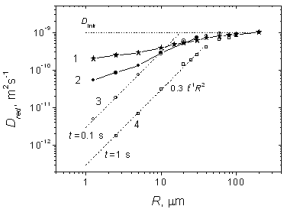

Figure 3. Reduced diffusivity as the function of R.

References

[1] P. N. Sen and P. J. Basser, *Magn. Reson. Imaging,* **23**, 215-220, 2006; [2] Y. Assaf and P. J. Basser, *NeuroImage,* **27**, 48-58, 2005; [3] F. Grinberg, In "Magnetic Resonance Microscopy", S. Codd and J. D. Seymour (Eds.), Wiley_VCH, Weinheim, p. 566, 2008.